2023 62nd IEEE Conference on Decision and Control (CDC)
December 13-15, 2023. Marina Bay Sands, Singapore

Experimental results for a pressure reducer control with a modular actuator*

Yassine Ariba[1], Frédéric Gouaisbaut[2], Flavien Deschaux[3], François Roux[4] and François Dugué[4]

***Abstract*— This paper addresses the control of a pressure regulator which reduces the pressure from an upstream chamber to a desired lower pressure in a downstream one. Most results in the literature, either neglect the actuator dynamic embedded in the reducer, or develop a specific design dedicated to their system. In this study, we propose to take into account this inner dynamic with a control system designed independently. The objective is to enable a modular architecture. It also justifies classical cascade control approach. A modeling work of the physical system combined with some practical assumptions provides a simple linear model. An output feedback control is designed to ensure stability, performance requirements and to cope with a saturation nonlinearity. Robust analysis approach and sector condition are used to address this feature as well as to take into account the dynamic of the independent controlled actuator with reduced assumptions on this subsystem. Stability condition of the overall system is expressed with LMI tests. Simulation and experimental tests show the validity of the proposed methodology.**

I. INTRODUCTION

Pressure regulation is an essential aspect of many industrial and technical processes. It involves controlling the pressure of a fluid or gas within a system to ensure optimal performance and safety. Pressure regulation is used in a wide range of applications, from medical systems [16], water supply networks [2], drilling mechanism [15] to chemical processing and automotive engine [6], [14], [1], [7]. In this context, many control laws have been developed in an ad hoc way, often taking into account the characteristics of the overall pressure system in order to maintain the stability of the operating point despite pressure calls from external environment. Various methods can be found, as the simplest control laws such as PI or PID, which are effective for linearized models around the operating points [8], [14], as well as more advanced control laws such as LQR, sliding mode [9], [7], backstepping [16] or switched control laws [15]. These control laws allow to take into account some nonlinearities that are common to many pressure control systems, such as saturation of the inlet flow valve or to make the closed loop system robust to external disturbances. However, in many works [2], the dynamic of the servo motor that drives the valve, and thus the flow, are not taken into account.

*This work was partly supported by the company CSTM and the CNES, the french national space agency.

[1]Y. Ariba is with the laboratory LAAS-CNRS, Université de Toulouse, INSA, Toulouse, France yariba@laas.fr

[2]F. Gouaisbaut is the laboratory LAAS-CNRS, Université de Toulouse, UPS, Toulouse, France fgouaisb@laas.fr

[3]F. Deschaux is with the company Comat, 31130 Flourens, France f.deschaux@comat.space

[4]F. Roux and F. Dugué are with the company CSTM, 31320 Castanet-Tolosan, France contact@cstm.fr

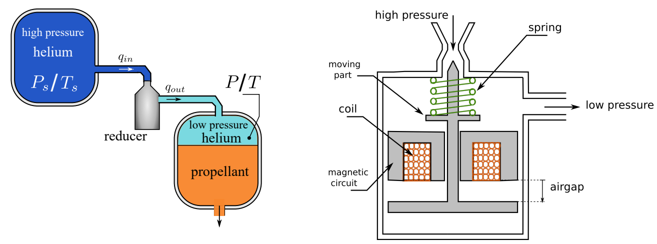

(a) (b)

Fig. 1: *(a) Launcher application and (b) Principle schematic of the pressure reducer / actuator.*

In this paper, we are interested in the design of a control law for an experimental pressure reducing device. The application context concerns an actuator for pressure control on a launcher. These regulators are used to expand helium from tanks at 400 bar to lower pressures (from a few bars to a few tens of bar) depending on the equipment requirements. They are in particular in charge of the pressurization of the propellant tank and thus ensure the injection in the combustion chamber (see Figure 1a for a simplistic principle scheme). Currently, the regulators are mechanical/pneumatic technologies and are passive. The development of an innovative electronic regulator [13], [3], which will be digitally controlled, with an adapted control system, will make it possible to maintain a constant downstream pressure despite disturbances (flow calls, temperature, vibrations) [12].

The proposed control law is designed independently of the actuator dynamics. However, the study of the stability of the operating point is carried out by taking into account the dynamics of a generic actuator, admitting a limited number of assumptions, especially the existence of a Lyapunov function for the set point of the actuator. Finally, the proposed methodology is illustrated on simulations and an experiment on a test bench is conducted to compare results and to validate the methodology.

II. SYSTEM MODELING

A. Description of the reducer

A principle schematic of the pressure reducer with the actuator is given in Figure 1b. As illustrated, in our work and testbed, an electromagnetic actuator is used to control the valve position. Nevertheless, this study aims at designing a control law for the pressure reducer independently of the technology of the positioning system. This objective

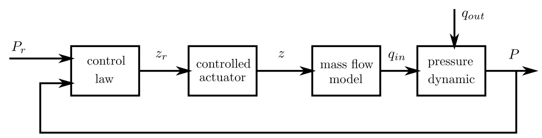

Fig. 2: *Block diagram of the feedback control system.*

Symbols	Description	Units
P_s	Supply pressure (high)	Pa
P	Downstream pressure (to be regulated)	Pa
T_s	Temperature in the supply tank	K
T	Temperature in the downstream chamber	K
V	Volume of the downstream chamber	m^3
q_{in}	Inlet flow rate	g/s
q_{out}	Oulet flow rate	g/s
m	Mass of the gas	g
M	Molar mass	g mol^{-1}
n	Amount of substance	mol
R	Ideal gas constant	J mol^{-1} K^{-1}
R_{spec}	Specific gas constant = R/M	J K^{-1} g^{-1}

TABLE I: Nomenclature for key variables/parameters.

is to allow a modular architecture which is interesting for reusability of equipment and to simplify the control design (as in cascade control approach). We intend then to prove the overall stability property with reduced knowledge on the controlled actuator/servomotor. The structure of the system is depicted in Figure 2. Basically, the actuator controls the position of a moving mechanical part, which itself changes the fluid flow rate (a gas in our application), modifying the opening of the flow cross section, from a upstream chamber to a downstream one.

B. Modeling

Applying thermodynamical laws, an analytical model is proposed for the pressure dynamic. To this end a set of general assumptions are made, and particularly relevant for the launcher application.

Assumption 1: (a) In the studied application, we always have $P_s/P > 2$, hence sonic flow is considered. (b) The ideal gas law can be applied. (c) The gas expansion and compression are adiabatic transformations. It implies there is no heat transfer between the system and its environment. (d) The temperature of the gas downstream of the actuator is constant. Experiments on our setup have shown that the temperature decreased very slightly and this phenomenon can be neglected.

By Assumption 1b, let us invoke the ideal gas law, we have at the downstream side of the actuator: $PV = nRT$ where all variables and parameters are defined in Table I and depicted in Figure 1a. Introducing the mass of the gas $m = nM$ and its specific gas constant $R_{spec} = R/M$, the law is rewritten as: $PV = mR_{spec}T$. Differentiating the latter equation,

$$V\frac{dP}{dt} = R_{spec}T\frac{dm}{dt},$$

and considering that the mass variation $\dot{m}$ can be modeled by the difference of the mass flow rate $q_{in} - q_{out}$, a dynamic model for the pressure is obtained:

$$\dot{P} = k\Big(q_{in} - q_{out}\Big) \tag{1}$$

with $k = \frac{R_{spec}T}{V}$. This latter is constant by Assumption 1d. This modeling approach allows us to derive a simple integrator model.

The inlet flow is controlled by a positioning actuator that modifies the cross-sectional area at the bottleneck S_{in}. Because the flow is sonic (Assumption 1a), the mass flow rate does not depend on the downstream pressure P. Using the relationships of an adiabatic process (Assumption 1c), the mass flow rate equals

$$q_{in} = \rho_s\left(\frac{2}{\gamma+1}\right)^{\frac{1}{\gamma-1}} S_{in}(z)\sqrt{2\gamma R_{spec}\frac{T_s}{\gamma+1}}$$

The function $S_{in}(z)$ is defined by the mechanical design of the valve needle and the seat. In practice, analytical calculation to establish the relationship between z and S_{in} is very complicated because of the complex neck shape designed from fluid mechanics requirements. Numerical simulations have been therefore conducted with a mechanical engineering Computer-Aided Design software to measure the cross-sectional area for different positions of the needle and to derive a two order polynomial approximation. Upstream parameters ρ_s and T_s being considered as constant over the duration of an experiment, all coefficients can be lumped with the polynomial coefficients of $S_{in}(z)$. Finally, one obtain a model for the mass flow block in Figure 2, a static function of the form:

$$q_{in} = f_{bn}(z) = c_2z^2 + c_1z + c_0 \tag{2}$$

with c_i being known constant parameters that mainly depend on the design of the bottleneck and the supply tank state. However, the opening area is necessarily limited and it thus saturates the flow. Let us define $sat_1(\cdot)$ an asymmetric saturation function such that

$$sat_1(q_{in}) = \begin{cases} q_{\min} & \text{if} \quad q_{in} < q_{\min} \\ q_{in} & \text{if} \quad q_{\min} < q_{in} < q_{\max} \\ q_{\max} & \text{if} \quad q_{in} > q_{\max} \end{cases} \tag{3}$$

Assumption 2: The static function f_{bn} modeling the relationship between the needle position and the mass flow is assumed to be a monotonically increasing function. Furthermore, regarding the inverse function, it is also assumed that there exist α, a known positive scalar such that:

$$\left|f_{bn}^{-1}(x_2) - f_{bn}^{-1}(x_1)\right| \leq \alpha\left|x_2 - x_1\right|$$

It is thus required $f_{bn}^{-1}(\cdot)$ to be locally Lipschitz on the operation range.

III. Control law design

A. Control law design without the actuator dynamics

At this stage, we consider the design of a control law without taking into account the actuator controlling the position of the valve. In that case, the pressure dynamic is modeled by equation (1) with q_{in} being the (virtual) control input. The key idea is to simplify the control design by decoupling subsystems, and to lead to a modular approach. Let us add an extra state variable, as the integral of the difference between the setpoint and the measure, to include an integral effect in the control law to reject constant disturbances and ensure a zero static error. Then, we define a state space model as follows, with $x_1 = P$ and $x_2 = \int_0^t P(\theta) - P_{ref}\ d\theta$,

$$\begin{cases} \dot{x}_1 = & k\Big(sat_1(q_{in}) - q_{out}\Big) \\ \dot{x}_2 = & x_1 - P_{ref} \end{cases}$$

Applying a state feedback control of the form $q_{in} = k_1(x_1 - P_{ref}) + k_2 x_2$, the unique equilibrium point is $x_{eq} = [P_{ref}\ \ q_{out}/k_2]^T$. Defining the error state vector $e = x - x_{eq}$, the closed-loop error dynamic is described by

$$\begin{cases} \dot{e}_1 = & k\Big(sat_1(k_1 e_1 + k_2 e_2 + q_{out}) - q_{out}\Big) \\ \dot{e}_2 = & e_1 \end{cases} \quad (4)$$

Note that, the region of linearity for the above system is defined by the set

$$\mathcal{R}_L = \Big\{ e \in \mathbb{R}^2 \mid \underbrace{q_{\min} - q_{out}}_{<0} \leq k_1 e_1 + k_2 e_2 \leq \underbrace{q_{\max} - q_{out}}_{>0} \Big\}$$

For $e \in \mathcal{R}_L$, system (4) with error coordinates is merely a second order linear system and state feedback gains k_1 and k_2 can easily be designed to ensure local stability around the origin as well as desired performance requirements. We aim at taking into account the saturation phenomenon and better estimate the region of stability of the setpoint equilibrium.

Inspired from [10], let define the dead-zone function $\phi(\theta) = sat_1(\theta + q_{out}) - \theta - q_{out}$ so as to reformulate system (4) into

$$\dot{e} = \underbrace{\begin{bmatrix} kk_1 & kk_2 \\ 1 & 0 \end{bmatrix}}_{A} e + \underbrace{\begin{bmatrix} k \\ 0 \end{bmatrix}}_{B} \phi(Ke) \quad \text{with } K = \begin{bmatrix} k_1 & k_2 \end{bmatrix} \quad (5)$$

Note that it is asymmetric w.r.t. the ordinate axis and the dead-zone range depends on the outflow rate q_{out}. Even though, this latter can be seen as a disturbance for the pressure control, its presence is necessary to include the origin in the linear mode of system (5).

At this stage, the generalized sector condition can be applied to cope with the nonlinear term in (5). Let define the set

$$S(K - G, q_{\min} - q_{out}, q_{\max} - q_{out}) = \Big\{ e \in \mathbb{R}^2 \mid q_{\min} - q_{out} \leq (K - G)e \leq q_{\max} - q_{out} \Big\}$$

where matrix $G \in \mathbb{R}^{1\times 2}$ is a free matrix that will define the sector, and thus the region of attraction to be estimated. The corresponding sector condition is

$$\phi(Ke)^T M \Big(\phi(Ke) + Ge \Big) \leq 0$$

with M any positive scalar. Then, from the above condition a theorem for the local asymptotic stability of (5) can be stated.

Theorem 1: For given gains k_1 and k_2 such that matrix A in (5) is Hurwitz. If there exist a matrix $Z \in \mathbb{R}^{1\times 2}$, a scalar $U > 0$ and a positive definite matrix $W \in \mathbb{R}^{2\times 2}$ such that

$$\begin{pmatrix} WA^T + AW & BU - Z^T \\ UB^T - Z & -2U \end{pmatrix} < 0$$

and

$$\begin{pmatrix} W & WK^T - Z^T \\ KW - Z & u_0^2 \end{pmatrix} \geq 0$$

where $u_0^2 = \min\Big\{ (q_{\min} - q_{out})^2, (q_{\max} - q_{out})^2 \Big\}$, then the origin for the system (5) is locally asymptotically stable (LAS). The region of attraction is estimated by the ellipsoid

$$\varepsilon(X, 1) = \big\{ e \in \mathbb{R}^2 \mid e^T X e \leq 1 \big\} \qquad \text{with} \qquad X = W^{-1}$$

Proof: The proof is similar to [11], [10] and only a sketch is proposed. The proof is based on the use of a quadratic Lyapunov function $V(e) = e^T X e$. The first LMI is derived from the definite negativeness condition for the Lyapunov function derivative along the trajectories of (5), while the second one defines the ellipsoid that is included in the polyhedral set $S(K - G, q_{\min} - q_{out}, q_{\max} - q_{out})$. The decision variables Z and U correspond, respectively, to GW and M^{-1}. Differently from [10], we have adapted the definition of parameter u_0 to cope with the asymmetric feature of the saturation. ■

B. Taking into account the actuator dynamics

Most results in the literature, either neglect the actuator dynamic that controls the valve opening, or develop a specific design dedicated to their setup. Such actuators may be autonomous systems that are controlled independently from the usage. In this paper, a modular approach is proposed where the control laws of the actuator and the pressure reducer are designed separately. Then, the overall stability must be analyzed. The actuator used in our pressure regulator is an electromagnetic actuator that drives the valve with a linear motion [5]. Generally speaking, the closed-loop model for the controlled actuator could be of the form

$$\begin{cases} \dot{\eta} = f_a(\eta, z_r) \\ \delta z = C_a \eta \end{cases} \quad (6)$$

where the state η corresponds to the error coordinates of the actuator state variables (typically, the valve position, the velocity and the coil current) w.r.t. the equilibrium point and the reference signal z_r. Its dynamic is nonlinear in general. Only the output $\delta z = z - z_r$ is assumed to be linear in the state η. It is thus considered that a previous study has designed a control law that ensures the asymptotic stability of (6) and the convergence of z toward z_r.

Assumption 3: It is assumed that the origin of system (6) is the unique equilibrium point, $\forall z_r \in \mathbb{R}$, and is asymptotically stable. Thus, z converges toward the desired reference z_r. It is also assumed that a Lyapunov function $V_a(\eta)$ for the aforementioned system is known and is such that $\dot{V}_a(\eta) \leq -\eta^T Q_a \eta$, with $Q_a \in \mathbb{R}^{n_a \times n_a}$ a positive definite matrix.

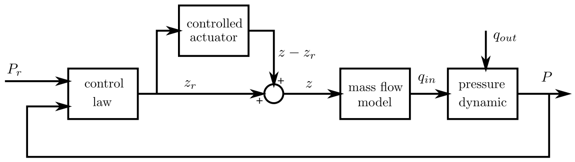

Fig. 3: *Block diagram of the feedback control system emphasizing the position deviation δz.*

Let redraw the block diagram in Figure 2 into the one in Figure 3 to emphasize the impact of the deviation of the actual actuator position from the ideal one. This latter correspond to the control law as designed in the previous section $z_r = f_{bn}^{-1}\big(Ke+q_{out}\big)$ where $f_{bn}^{-1}(\cdot)$ is the reciprocal function of $f_{bn}(\cdot)$ in (2). Hence, the potential inlet flow rate is now expressed as:

$$\begin{aligned} q_{in} =& f_{bn}\Big(z_r+\delta z\Big) = f_{bn}\Big(f_{bn}^{-1}\Big(Ke+q_{out}\Big)+\delta z\Big) \\ =& f_{bn}\Big(f_{bn}^{-1}\Big(Ke+q_{out}\Big)\Big) + c_2\delta z^2 \\ & + 2c_2\delta z \underbrace{f_{bn}^{-1}\Big(Ke+q_{out}\Big)}_{z_r} + c_1\delta z \\ =& Ke + q_{out} + \delta z \underbrace{\Big(c_2\delta z + 2c_2 z_r + c_1\Big)}_{\Delta} \end{aligned}$$

In that case, the error system (4) is expressed as

$$\begin{cases} \dot e_1 = & k\Big(sat_1(Ke+q_{out}+\delta z\Delta) - q_{out}\Big) \\ \dot e_2 = & e_1 \end{cases} \qquad (7)$$

Clearly, when the position deviation δz is set to 0, the model of the previous section is recovered. The new region of linearity for the above system is now defined by

$$\mathcal{R}_L = \Big\{ e\in\mathbb{R}^2 \mid q_{\min}-q_{out} \le Ke+\delta z\Delta \le q_{\max}-q_{out} \Big\}$$

Let us model Δ as a bounded uncertain parameter and define the augmented state ξ and gain $\bar K$:

$$\Delta\in[\Delta_1\ ,\ \Delta_2] \quad \xi = \begin{bmatrix}\eta\\ e\end{bmatrix} \quad \text{and} \quad \bar K = \begin{bmatrix}\Delta C_a & K\end{bmatrix} \qquad (8)$$

The same dead-zone function $\phi(\theta)$ is proposed but with a different argument $\theta = Ke + \delta z\Delta = \bar K\xi$. Combining (6) and (7), the whole pressure reducing system, including the valve control dynamic, can be expressed as

$$\begin{cases} \dot\eta = f_a(\eta, z_r) \\ \dot e = \underbrace{\begin{bmatrix} kk_1 & kk_2 \\ 1 & 0\end{bmatrix}}_{A} e + \underbrace{\begin{bmatrix} k\Delta C_a \\ 0\end{bmatrix}}_{B_1}\eta + \underbrace{\begin{bmatrix} k\\ 0\end{bmatrix}}_{B}\phi(\bar K\xi) \end{cases} \qquad (9)$$

In order to deal with the nonlinear deadzone function, let redefine the set

$$\begin{aligned} & S(\bar K - G, q_{\min}-q_{out}, q_{\max}-q_{out}) = \\ & \Big\{\xi\in\mathbb{R}^{n_a+2} \mid q_{\min}-q_{out} \le (\bar K - G)\xi \le q_{\max}-q_{out}\Big\} \end{aligned}$$

where matrix $G\in\mathbf{R}^{1\times n_a+2}$ is a free matrix that defines the generalized sector condition

$$\phi(\bar K\xi)^T M\Big(\phi(\bar K\xi)+G\xi\Big) \le 0 \qquad (10)$$

with M any positive scalar. The following theorem proposes a stability condition for the pressure regulator when the actuator dynamic, for which the control system has been designed independently, is now taken into account.

Theorem 2: Under Assumptions 2 and 3, for given gains k_1 and k_2 such that matrix A in (9) is Hurwitz, and for given Δ_1 and Δ_2 defining the set Δ in (8), if there exist matrices $Z\in\mathbb{R}^{1\times 2}$ and $G_1\in\mathbb{R}^{1\times n_a}$, a scalar $U>0$ and a positive definite matrix $W\in\mathbb{R}^{2\times 2}$ such that

$$\begin{bmatrix} -Q_a & B_1(\Delta_i)^T & -G_1^T \\ B_1(\Delta_i) & WA^T+AW & BU-Z^T \\ -G_1 & UB^T - Z & -2U \end{bmatrix} < 0 \qquad (11)$$

for $i=\{1,2\}$ and

$$\begin{pmatrix} W & WK^T - Z \\ (WK^T-Z)^T & u_0^2 \end{pmatrix} \ge 0 \qquad (12)$$

where $u_0^2 = \min\Big\{(q_{\min}-q_{out})^2, (q_{\max}-q_{out})^2\Big\}$, then the origin for system (9) is locally asymptotically stable (LAS).

Proof: Consider the Lyapunov function candidate

$$V(\xi) = V_a(\eta) + e^T X e$$

with $X\in\mathbb{R}^{2\times 2}$ a positive definite matrix and V_a a Lyapunov function introduced in Assumption 3 and associated to the controlled actuator. Let us calculate its time-derivative:

$$\begin{aligned} \dot V(\xi) =& \ \dot V_a(\eta) + 2e^T X\dot e \\ \le& -\eta^T Q_a\eta + 2e^TXAe + 2e^TXB_1\eta + 2e^TXB\phi(\bar K\xi) \end{aligned}$$

$\forall\xi\in S(\bar K - G, q_{\min}-q_{out}, q_{\max}-q_{out})$, we have

$$\begin{aligned} \dot V(\xi) \le & -\eta^TQ_a\eta + 2e^TXAe + 2e^TXB_1\eta \\ & + 2e^TXB\phi(\bar K\xi) - 2\phi(\bar K\xi)^TM\Big(\phi(\bar K\xi)+G\xi\Big) \\ \le & \begin{bmatrix}\eta\\ e\\ \phi(\bar K\xi)\end{bmatrix}^T \Xi(\Delta) \begin{bmatrix}\eta\\ e\\ \phi(\bar K\xi)\end{bmatrix} \end{aligned}$$

with

$$\Xi(\Delta) = \begin{bmatrix} -Q_a & B_1(\Delta)^TX & -G_1^TM \\ XB_1(\Delta) & A^TX+XA & XB-G_2^TM \\ -MG_1 & B^TX - MG_2 & -2M \end{bmatrix}$$

and $G=[G_1\ G_2]$. Hence, proving $\Xi(\Delta)<0$, $\forall\Delta\in[\Delta_1\ ,\ \Delta_2]$, implies that $\dot V(\xi)$ is negative definite. Matrix $\Xi(\Delta)$ being linear in Δ, it is sufficient to test the condition on its bound as in polytopic approach. Consequently, if the two conditions: $\Xi(\Delta_1)<0$ and $\Xi(\Delta_2)<0$ are satisfied, then $\dot V(\xi)<0$ $\forall\xi\in S(\bar K - G, q_{\min}-q_{out}, q_{\max}-q_{out})\setminus\{0\}$ and $\dot V(0)=0$. In that case, function V is thus a Lyapunov function for system (9) and the LAS of the origin is proven. By left and right multiplying both $\Xi(\Delta_i)$ by diag$(\mathbb{I}_{n_a}, X^{-1}, M^{-1})$ and denoting $U=M^{-1}$, $X^{-1}=W$

and $Z = G_2 W$, the conditions are LMI, which can be tested efficiently. ■

In a second step, the second LMI (12) in Theorem 2 defines an ellipsoidal set for e

$$\varepsilon(X, 1) = \{e \in \mathbb{R}^2 \mid e^T X e \leq 1\} \quad \text{with } X = W^{-1}$$

that is included in the polyhedral $S(\bar{K} - G, q_{\min} - q_{out}, q_{\max} - q_{out})$. The limit of this ellipsoidal set corresponds to a level curve for the projection of the Lyapunov function $V(\xi)$ on the e plane. It could thus provide an estimation of the basin of attraction w.r.t. state variable e. However, the uncertain parameter

$$\Delta = c_2 \delta z + 2c_2 z_r + c_1 = c_2 \delta z + 2c_2 f_{bn}^{-1}(Ke + q_{out}) + c_1$$

depends on e and η, and was assumed to be bounded. It is required to make sure to select Δ_1 and Δ_2 such that for all $e \in \varepsilon$, it implies that $\Delta \in [\Delta_1 \ , \ \Delta_2]$. So that the uncertain modeling does not affect the region of attraction. The conditions are stated in the following proposition.

Proposition 1: For a given nominal q_{out} and for a given maximal deviation $\bar{\delta z}$, if Theorem 2 and the two inequalities, parameterized by Δ_1, Δ_2 and X,

$$\Delta_1 \leq 2c_2 f_{bn}^{-1}(q_{out}) + c_1 - |c_2 \bar{\delta z}| - 2\alpha |c_2| \, \|K\| \frac{1}{\sqrt{\lambda_{\min}(X)}}$$

$$\Delta_2 \geq 2c_2 f_{bn}^{-1}(q_{out}) + c_1 + |c_2 \bar{\delta z}| + 2\alpha |c_2| \, \|K\| \frac{1}{\sqrt{\lambda_{\min}(X)}}$$

are satisfied, then an inner estimation of the basin of attraction is given by the ellipsoidal set

$$\varepsilon(X, 1) = \{e \in \mathbb{R}^2 \mid e^T X e \leq 1\} \quad \text{with } X = W^{-1} \tag{13}$$

where W is obtained from the resolution of the aforementioned LMI (12).

Proof: The proof is omitted due to space limitation. It is detailed in the submitted version available on the HAL platform. ■

IV. Simulation and Experimental Results

This section presents simulation with MATLAB/Simulink and experimental results. Numerical values for system parameters are not given for confidentiality reasons.

A. Simulations

Considering (5), consisting of the physical model and an integral action, the state feedback gain K has been designed with the classical pole placement method to ensure A is hurwitz and have the dead-zone free system converging in approximately 2 seconds. Then, Theorem 2 is applied to prove that the whole system ((5) + flow rate saturation + static function f_{bn} + actuator dynamic) is LAS. Let us consider a linear servomotor, asymptotically stable and for which the derivative of the Lyapunov function is bounded by a quadratic form with $Q_a = 300\mathbb{I}_3$ (see Assumption 3). Regarding Assumption 2, the CAD model provides numerical values for the bottleneck function f_{bn} (2) and the bound α was computed $\alpha = 0.013\, mm/g/s$. The LMI (11)-(12) were tested with the objective function trace$(-W)$ so as to

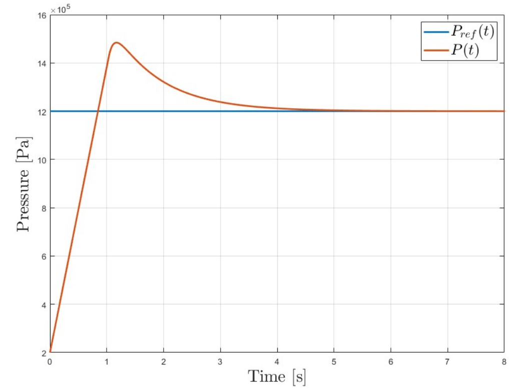

Fig. 4: *Time responses of the output pressure $P(t)$ (in ref) and the reference P_{ref} (in blue).*

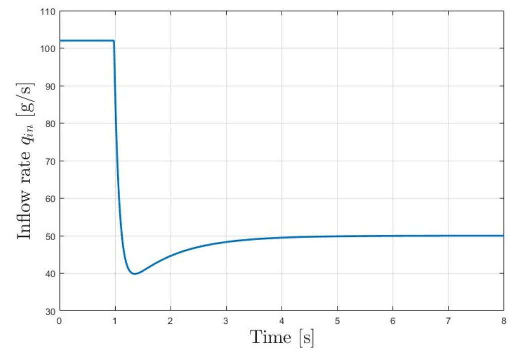

Fig. 5: *Time evolution of the (virtual) control input, that is the inflow rate $q_{int}(t)$.*

maximize the size of the ellipsoidal set ε and enlarge the estimation of the basin of attraction. First, a simulation is performed with an outflow rate $q_{out} = 50\, g/s$ and an initial condition $P(0) = 2\ bar$. The supply pressure, upstream of the actuator, is 50 bar while the desired downstream pressure P_{ref} is 12 bar. Figure 4 shows the time response of the output pressure $P(t)$ and P_{ref} its reference. As expected, the pressure converges to the desired setpoint. It can be seen that for approximately 1 s the system is in saturation mode. The virtual control input q_{int}, that is the inflow rate driven by the actuator, is shown in Figure 5. Because the initial pressure is low, the control law asks for maximal rate, limited by $q_{\max} = 102\ g/s$. As expected, at the steady state q_{in} equals q_{out} to balance the output flow and keeps the pressure constant.

B. Experimentation

For the experimental test, the setup parameters are quite similar to those of the simulation test. The outlet flow rate is time-varying with a piecewise constant profile:

$$q_{out}(t) = \begin{cases} 53 & g.s^{-1} & 0 \leq t < 5 \\ 74 & g.s^{-1} & 5 \leq t < 10 \\ 98 & g.s^{-1} & 15 \leq t \end{cases} \tag{14}$$

These changes are due to the application operational requirements downstream the pressure reducer system. The

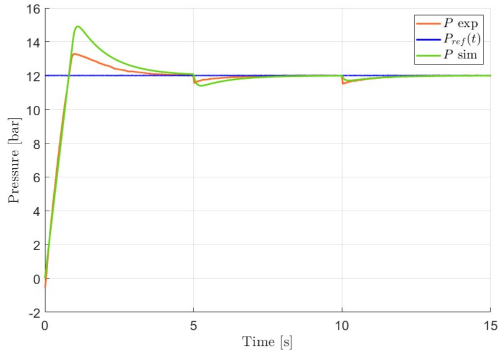

Fig. 6: *Time response of the output pressure $P(t)$: comparison between simulation (in green) and experimentation (in orange) results.*

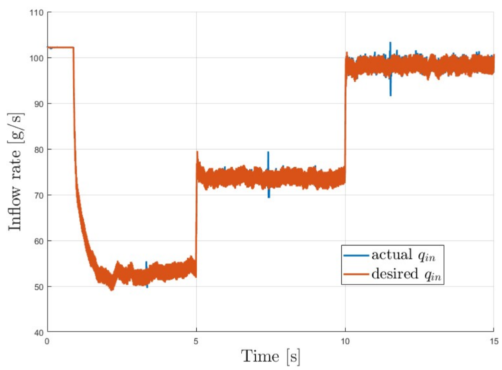

Fig. 7: *Time evolution of the (virtual) control input $q_{int}(t)$: comparison between the desired inflow rate (in orange) and the actual one (in blue).*

positioning actuator embedded in the testbed is an electromagnetic actuator[1] for which the control system was designed independently and ensures global asymptotic stability and a fast time response (about few milliseconds) [4], [5]. Experimental results are plotted in Figure 6 and 7. It shows that the proposed control system regulates the output pressure P to the desired value, despite the changes of the outlet flow rate (14). In Figure 7, experimental results are compared to simulation one. The behaviors are fairly similar and it validates the modeling approach. Figure 7 compares the desired inflow rate $q_{in} = f_{bn}(z_r)$ and the actual one $q_{in} = f_{bn}(z)$. The difference stems from the error dynamic of the actuator.

V. Conclusion

The physical modeling and the control of a pressure reducing system is proposed in this work. An output feedback with an integral action is developed to ensure local asymptotic stability while taking into account the inflow rate saturation. We also take into account the dynamic of the actuator, integrated in the pressure reducer, that controls the valve position in a decoupled way. The objective was to justify the usual cascade control approach, with an independent design between subsystems while guaranteeing the stability of the overall system. The stability analysis is expressed with LMI conditions and an estimation of the basin of attraction is also provided. The proposed control system was validated through experimental tests on a testbed with dry air.

[1] Also designed by the company CSTM

Acknowledgment

The authors are grateful to Damien De Seze from CNES and François Dugué from CSTM for the grants that have supported this activity.

References

[1] W. Birk and A. Medvedev. Pressure and flow control of a pulverized coal injection vessel. *IEEE Transactions on Control Systems Technology*, 8(6):919–929, 2000.

[2] C. De Persis and C. S. Kallesoe. Pressure regulation in nonlinear hydraulic networks by positive and quantized controls. *IEEE Transactions on Control Systems Technology*, 19(6):1371–1383, 2011.

[3] F. Deschaux, Y. Ariba, F. Gouaisbaut, D. DeSeze, and F. Dugué. Procédé de commande d'un actionneur éléctromagnétique pour un détendeur, March 2023. Patent number: FR3121193 / WO2022200710.

[4] F. Deschaux, F. Gouaisbaut, and Y. Ariba. Nonlinear control for an uncertain electromagnetic actuator. In *2018 IEEE Conference on Decision and Control (CDC)*, pages 2316–2321, 2018.

[5] F. Deschaux, F. Gouaisbaut, and Y. Ariba. Magnetic force modelling and nonlinear switched control of an electromagnetic actuator. In *2019 IEEE 58th Conference on Decision and Control (CDC)*, pages 1416–1421, 2019.

[6] X. Fan, Y. He, P. Cheng, and M. Fang. Fuzzy-type fast terminal sliding-mode controller for pressure control of pilot solenoid valve in automatic transmission. *IEEE Access*, 7:122342–122353, 2019.

[7] W. Han, L. Xiong, and Z. Yu. Interconnected pressure estimation and double closed-loop cascade control for an integrated electrohydraulic brake system. *IEEE/ASME Transactions on Mechatronics*, 25(5):2460–2471, 2020.

[8] M. Liermann. Pid tuning rule for pressure control applications. *International Journal of Fluid Power*, 14(1):7–15, 2013.

[9] H. Sun, L. Gao, Z. Zhao, and B. Li. Adaptive super-twisting fast nonsingular terminal sliding mode control with eso for high-pressure electro-pneumatic servo valve. *Control Engineering Practice*, 134:105483, 2023.

[10] S. Tarbouriech, G. Garcia, J. Silva, and I. Queinnec. *Stability and Stabilization of Linear Systems with Saturating Actuators*. Springer London, 01 2011.

[11] S. Tarbouriech, C. Prieur, and J.M.G. da Silva. Stability analysis and stabilization of systems presenting nested saturations. *IEEE Transactions on Automatic Control*, 51(8):1364–1371, 2006.

[12] P. Tatiossian, F. Dugué, and F. Roux. Electronic pressure regulator for liquid propulsion rockets. In *Space Propulsion*, Roma, Italy, May 2016.

[13] P. Tatiossian, F. Dugué, G. Jeanblanc, M. Pons, and H. Siguerdidjane. Détendeur à commande électronique, June 2015. Patent number: FR3007855.

[14] Q. Wang, H. Yao, Y. He, Y. Yu, and J. Yang. Research on rail pressure control of high-pressure common rail system for marine diesel engine based on controlled object model. *IEEE Access*, 9:125384–125392, 2021.

[15] J. Zhou, O. N. Stamnes, O. M. Aamo, and G.-O. Kaasa. Switched control for pressure regulation and kick attenuation in a managed pressure drilling system. *IEEE Transactions on Control Systems Technology*, 19(2):337–350, 2011.

[16] H. Zhuang, Q. Sun, Z. Chen, and Y. Jiang. Back-stepping sliding mode control for pressure regulation of oxygen mask based on an extended state observer. *Automatica*, 119:109106, 2020.